IN: Fire and Polymers II: Materials and Test for Hazard Prevention, American Chemical Society, ACS Symposium Series 599, August 21-26, 1994, Washington, DC

Chapter 11

Thermal Decomposition Chemistry of Poly(vinyl alcohol)

Char Characterization and Reactions with Bismaleimides

Jeffrey W. Gilman[1], David L. VanderHart[2], and Takashi Kashiwagi[1]

[1]Building and Fire Research Laboratory and [2]Materials Science and Engineering Laboratory, National Institute of Standards and Technology, Gaithersburg, MD 20899-0001

The fundamental condensed phase processes which lead to char formation during the fire-like pyrolysis of poly(vinyl alcohol), PVA, and PVA-containing maleimides were characterized using CP/MAS ^{13}C NMR. In addition to evidence of the well known chain-stripping elimination of H_2O and the chain-scission reactions, which occur during the pyrolysis of pure PVA, evidence is presented in support of cyclization and radical reaction pathways responsible for the conversion of unsaturated carbons into aliphatic carbons. Two general mechanisms; one described as a physical encapsulation, and the other a lowering of the average volatility of certain degradation products, are proposed for the primary modes of action of maleimides on the pyrolysis of PVA.

Currently, due to concerns over the environmental effects of halogenated compounds, there is an international demand for the control of polymer flammability without the use of halogenated additives (*1,2*). An alternative to the use of halogenated fire retardants, which control flammability primarily in the gas phase, is to control polymer flammability by manipulating the condensed phase chemistry. Our approach is to increase the amount of char that forms during polymer combustion. Char formation reduces, through crosslinking reactions, the amount of small volatile polymer pyrolysis fragments, or fuel, available for burning in the gas phase; this, in turn reduces the amount of heat feedback to the polymer surface. The char also insulates the underlying virgin polymer. All of these effects combine to reduce polymer flammability.

The polymer we chose to investigate was poly(vinyl alcohol), PVA, because it is one of the few linear, non-halogenated, aliphatic polymers with a measurable (~ 4%) char yield. We have attempted to characterize the fundamental condensed phase processes and structures which lead to char formation during the fire-like pyrolysis of poly(vinyl alcohol) and then to use this information to design new strategies that do not use halogenated additives, but which increase char formation (*3,4*). Strategies for retarding the flammability of polymers through enhanced char formation require an

understanding of how char forms; therefore, characterization of the polymer at several intermediate stages of decomposition is necessary. The thermal decomposition of PVA has been studied previously both in the gas and condensed phases; however, only limited characterization of the pyrolysis residues exists (*5,6*). Typical TGA analysis of PVA (5 °C/min, N_2), in Figure 1, shows two regions, 300-325 °C and 400-425 °C, where the weight loss rate is reduced relative to the more active portions of the thermogram. The intermediate decomposition products present in these regions have better thermal stability than PVA. We set out to characterize the structure of these pre-chars, to determine how they form, and how we might enhance their stability.

Experimental

Poly(vinyl-alcohol) Pyrolysis: PVA (99.7% hydrolyzed with aqueous NaOH, Mn = 86,000, Mw = 178,000, Scientific Polymer Products) was purified by Soxhlet extraction (MeOH, 2h) to remove NaOAC and heated (70°C, 5h) to give a white granular crystalline powder (particle size 100-1000 um) (*7*). This powder retained 6-7% H_2O by ^1H NMR and elemental analysis.

Previous studies have shown that the elemental composition, char yield and physical structure of polymer char, in many systems, were independent of whether they were formed via pyrolysis in nitrogen, or combustion in air (*8*), therefore, PVA was pyrolyzed in a flow pyrolysis apparatus using a nitrogen atmosphere (< 50 ppm O_2). This experimental setup allows study of the condensed phase decomposition processes under fire-like conditions in the absence of gas phase oxidation.

We prepared pyrolysis residues using 1-2 gram samples of PVA, at several intermediate stages of thermal decomposition. Pyrolysis was carried out for 30 minutes at each of several temperatures (250°C, 300°C, 350°C, and 400°C). The PVA was spread ~1-2 mm deep on a 5 cm x 10 cm ceramic tray for each pyrolysis. Two experiments per sample were run and the results averaged. Run-to-run differences were less than 10% of the measured value.

Poly(vinyl-alcohol)/Maleimide Pyrolysis: The maleimides N,N'-1,4-phenylenedimaleimide (1,4-PDMI, 98%, Aldrich), N,N'-1,3-phenylenedimaleimide (1,3-PDMI, 97%, Aldrich) and N-phenylmalemide (PMI, 97%, Aldrich) were used as received. The PVA/maleimide mixtures were prepared by simply grinding the maleimides with PVA, using a mortar and pestle, to give the following combinations: PVA/1,3-PDMI (10% by weight, 2 mole %), PVA/1,4-PDMI (10% by weight, 2 mole %), and PVA/PMI (12% by weight, 2 mole %). Typical particle sizes were 10-1000 um.

This approach was used because of the difficulties associated with melt blending PVA, since it's decomposition temperature is 30-40 °C below it's melting point, and because of our aversion to any solvent blending techniques. Solvent blending could adversely effect both polymer stability and flammability by altering the physical state (e.g., crystallinity) of PVA; in addition polymer-solvent reactions might occur, or other physical effects due to solvent escape might take place. All of these effects could complicate interpretation. We anticipated that some mixing would take place in the molten state as the PVA mixtures were heated. The effectiveness of the maleimides as crosslinking agents for PVA of course would depend on this mixing.

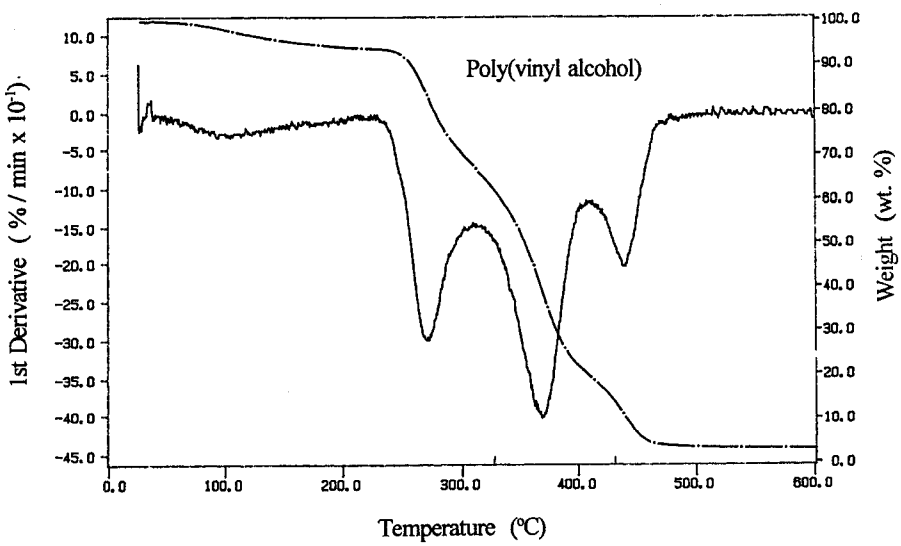

Figure 1. TGA of Poly(vinyl alcohol), 5 °C/min, broken line: weight loss vs. temperature, solid line: first derivative $\Delta\%/\Delta$ min. The plots reveal two regions, 300-325 °C and 400-425 °C, where the mass loss rate is slowed during degradation.

The mixtures were pyrolyzed in the N_2 flow pyrolysis furnace for 30 minutes at each of several temperatures (300 °C, 350 °C, and 400 °C). Two experiments per sample were run and the results averaged. Run-to-run differences for these pyrolyses were less than 4% of the measured values.

Characterization: Solid state ^{13}C NMR characterization utilized techniques of cross polarization (CP) and magic angle spinning (MAS) (25Mhz, 4Khz MAS, 1ms CP time, 3s rep. time) (*9*). In the decoupler blanking CP/MAS ^{13}C NMR experiments the decoupler was turned off for 40 us prior to sample observation with decoupling (*10*). Elemental analysis was also employed (Galbraith, two determinations per sample).

Results & Discussion

Poly(vinyl-alcohol) Pyrolysis: Upon heating PVA above the decomposition temperature the polymer begins a rapid chain-stripping elimination of H_2O shown in Figure 2 (*11,12*). This process coupled with melting causes the material to foam or intumesce as it decomposes. This and other decomposition reactions cause color changes and crosslinking to yield insoluble yellow to black rigid foam-like residues. The physical appearance, carbon-to-hydrogen ratio and residue yields were recorded for these pyrolyses (Table I).

Table I. PVA and Residues: Appearance, C/H Ratio and Yield

Material	Appearance	C/H Ratio	Residue Yield (%)
PVA	white granular solid	0.50	NA
Polymer residue 250 °C (30 min)	yellow-orange foam	0.52	82
Polymer residue 300 °C (30 min)	tan rigid foam	0.71	47
Polymer residue 350 °C (30 min)	dark brown foam	0.83	18
Polymer residue 400 °C (30 min)	black powder	1.00	5

Direct spectroscopic evidence of the chain-stripping elimination of H_2O was observed by comparison of the CP/MAS ^{13}C NMR spectra of PVA with the spectra of the residues. Figure 3 shows a progressive reduction in the intensity of the alcohol methine carbon (-CH(OH)-) signal at ~ 70 ppm as well as the growth of signals in the olefinic and aromatic region between 120 -140 ppm as the exposure temperature increases. The spectra of the residues all show methyl signals at 15 and 20 ppm. These

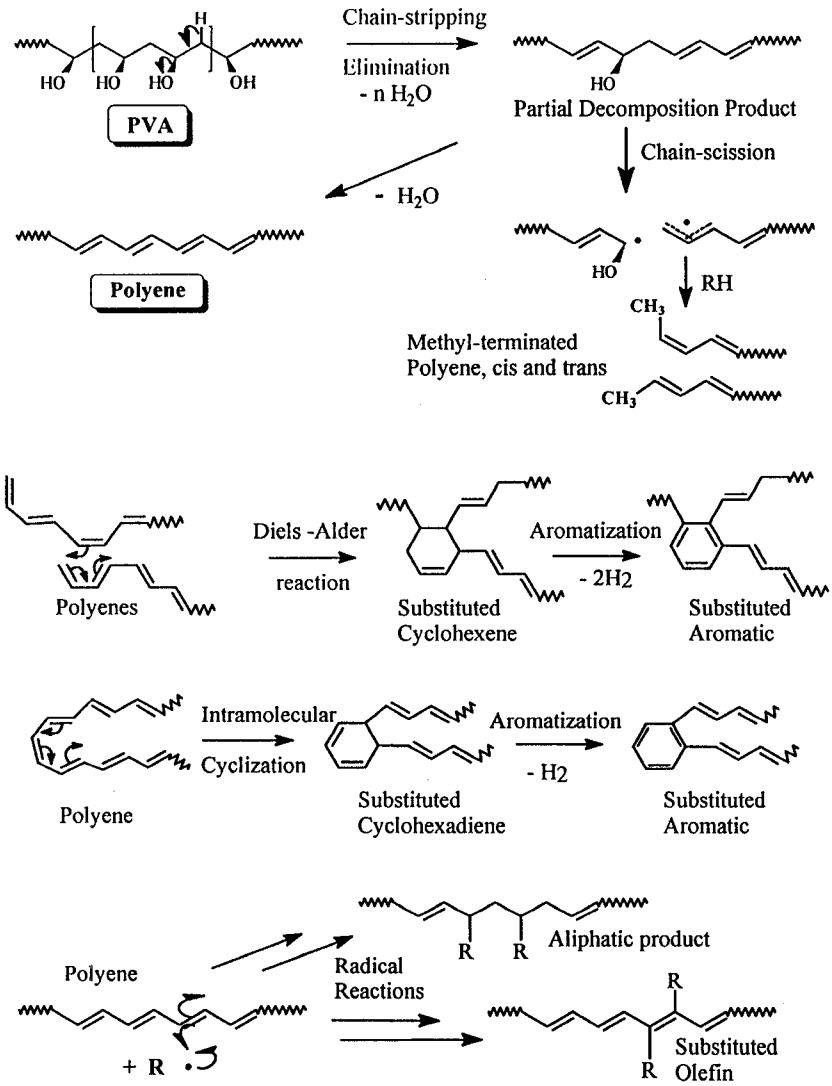

Figure 2. Proposed PVA pyrolysis reactions.

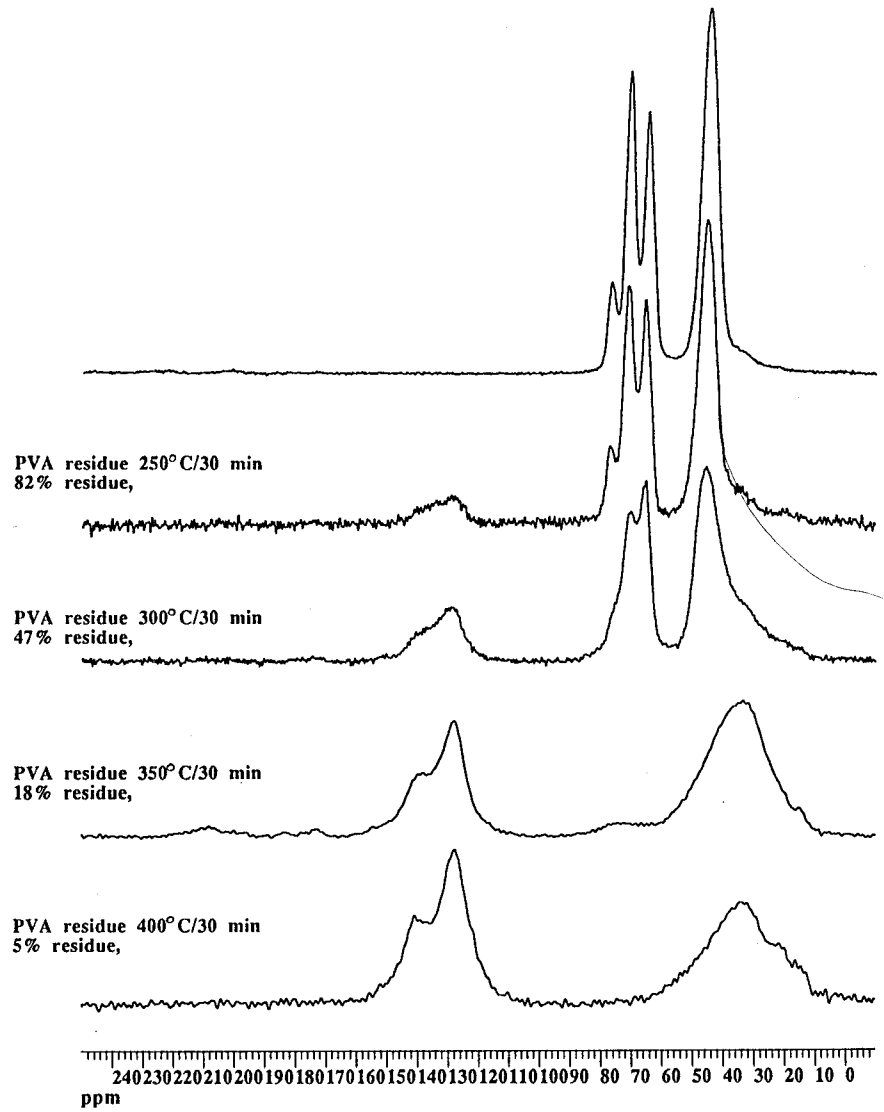

Figure 3. 25 MHz CP/MAS ^{13}C NMR spectra, normalized to the same total intensity, of PVA and PVA pyrolysis residues. Note the progressive loss of alcohol carbons (~70 ppm) and the corresponding gain in aromatic/olefinic carbons (110-150 ppm).

signals possibly arise from cis and trans allylic-methyls that may form via random chain scission reactions that can accompany elimination. This pyrolysis pathway is included in Figure 2.

At 350 °C the elimination reaction appears complete, most of the alcohol carbon signal at ~70 ppm (the fraction of alcohol-carbon intensity is only ~10% of that fraction in the original PVA) and the adjacent methylene signal at ~ 45 ppm are gone. In the 350 °C residue from integration 59% of the carbons are aliphatic (15-50 ppm). Moreover, the C/H ratio (table I) is 0.83, indicative of material that has a significant CH_2 and/or CH_3 component. It appears that at temperatures up to 350 °C the polyenes, from the elimination reaction, are converted into aliphatic groups (10-50 ppm). The Diels-Alder, intramolecular cyclization and radical reactions, shown in Figure 2, may be responsible for this conversion.

The Diels-Alder reaction has been proposed previously in a study of the acid catalyzed decomposition of PVA at 140 °C, and a similar intramolecular cyclization reaction has been proposed in the thermal decomposition of PVC (*13,14*). The Diels-Alder reaction, however, is the most efficient of the three processes at producing aliphatic carbons. It converts 4 of the 6 reacting sp^2 carbons into sp^3 carbons. The Diels-Alder and the intramolecular cyclization reactions produce substituted cyclohexenes and cyclohexadienes, respectively, that can aromatize to substituted aromatics.

To determine the extent to which carbon-carbon bond forming reactions, like those shown in Figure 2, occurred we employed a CP/MAS ^{13}C NMR interrupted decoupling experiment. This technique favors the observation of ~ 95% of the original intensity of the non-protonated carbons in a rigid sample; in addition about ~ 55% of the methyl carbon intensity also appears in these type of experiments. The result of applying this technique to the 350 °C residue, seen in Figure 4, shows that ~ 40% of the signal at 120-150 ppm in the normal CP/MAS spectrum is from non-protonated carbons, specifically, substituted olefinic or aromatic carbons. This indicates substantial carbon-carbon bond formation by reactions like those, shown in Figure 2, which form the substituted aromatics and or substituted olefinics. Substituted aromatics are of course the precursors to polynuclear aromatic structures found in char. Indeed, CP/MAS ^{13}C NMR analysis of PVA high temperature nitrogen-atmosphere pyrolysis char, shown in Figure 5, reveals that only these type of structures survive at high temperatures. Figure 4 also shows other non-protonated carbons, at 170 and 208 ppm, present in the 350 °C residue. The signal at 170 ppm may be assigned to the carbonyl carbon in carboxylic acid or anhydride groups and the signal at 208 ppm to ketones or the sp carbon of an allene (*15*). Further application of this technique revealed that the carbon-carbon bond formation reactions occur at temperatures as low as 250 °C producing substituted aromatic/olefinic carbons, see Figure 6, essentially concomitant with the chain-stripping elimination reaction. From Figure 7, we see that in the 400 °C residue ~50 % of all the carbons in the residue are aliphatic and almost all of the aliphatic carbons are still protonated. There is a strong implication of methine aliphatic carbon (CH) from these spectra. This is consistent with the overall C/H ratio of 1.00 (Table I) for the 400 °C residue, and supports the CH forming reactions shown in Figure 2 , i.e., the Diels-Alder reaction, intramolecular cyclization and radical reactions.

The reactions and products shown in Figure 2 illustrate the probable mode of PVA

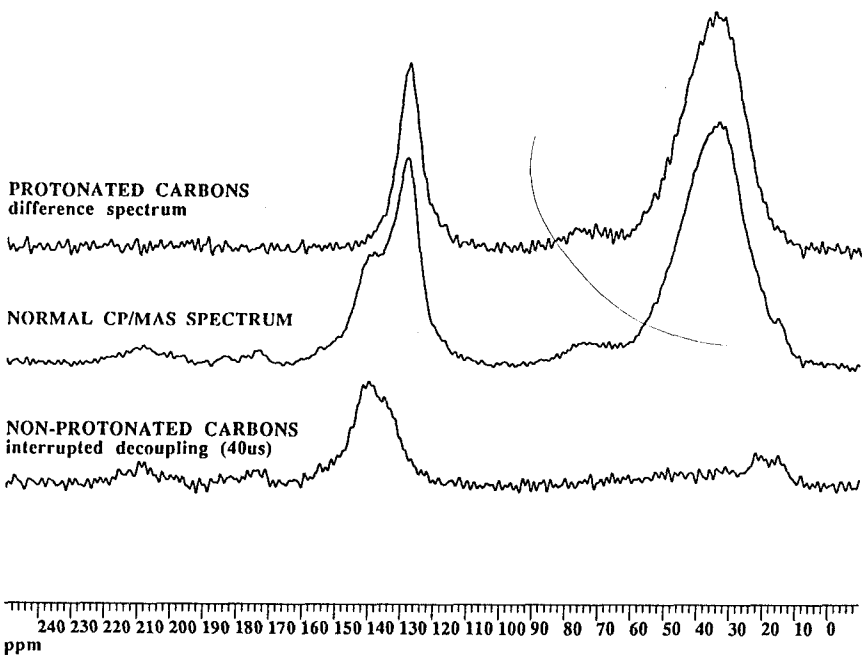

Figure 4. CP/MAS ^{13}C NMR spectra of residue of PVA pyrolyzed at 350 °C for 30 min. The spectrum of the non-protonated carbons and of a fraction (~55%) of the methyl carbons in the residue is obtained using the interrupted decoupling experiment (bottom). The difference spectrum (top) results from subtracting the non-protonated spectrum (bottom) from the normal CP/MAS spectrum (middle). The multiplication factor used in the subtraction is based on our knowledge of the average attenuation of a non-protonated carbon in the interrupted decoupling experiment.

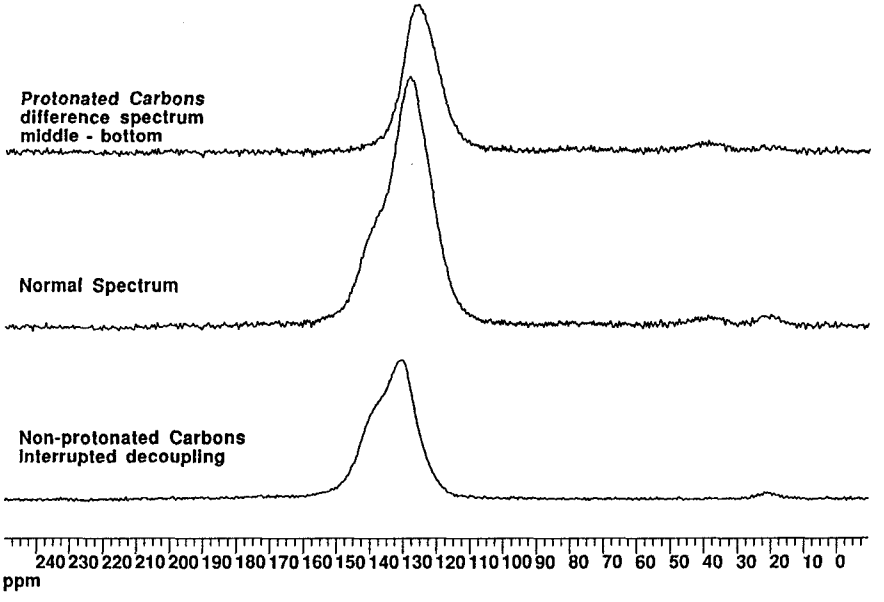

Figure 5. CP/MAS ^{13}C NMR spectra of char from pyrolysis of PVA in high temperature (700-800 °C) gasification apparatus under nitrogen. As in Figure 4 the spectrum of the protonated carbons (top) in the char was generated by subtracting the non-protonated spectrum (bottom) from the normal CP/MAS spectrum (middle). Note that the shape of the non-protonated carbon resonances differs from the corresponding shapes of the lower temperature residues (see Figures 4, 6 and 7); yet the fraction of protonated aromatic carbons is only modestly reduced at 800 °C, relative to the 350 °C and 400 °C residues.

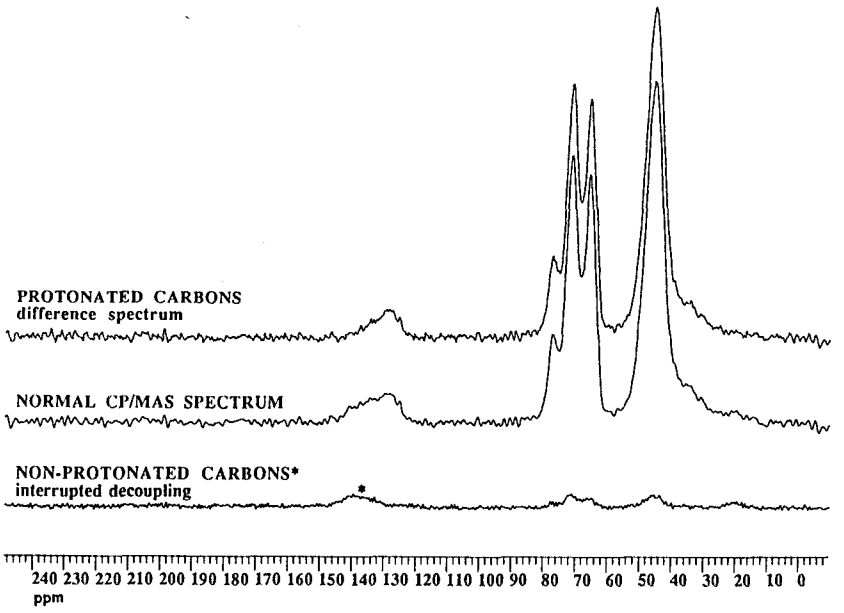

Figure 6. CP/MAS ^{13}C NMR spectra of residue of PVA pyrolyzed at 250 °C for 30 min. Interrupted decoupling spectrum (bottom) shows that even at 250 °C non-protonated carbons are present.

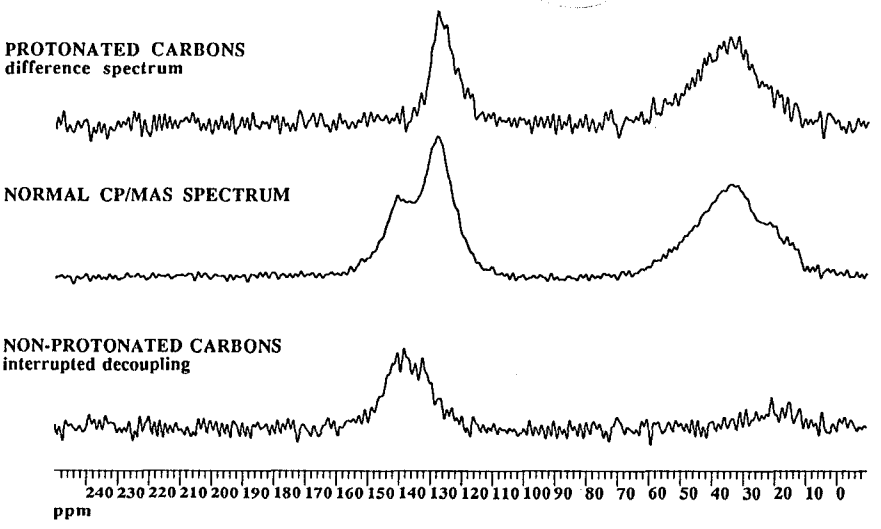

Figure 7. CP/MAS ^{13}C NMR spectra of residue of PVA pyrolyzed at 400 °C for 30 min (after Figure 4). Even at 400 °C a significant portion of the residue consist of protonated sp^3 carbons.

decomposition initially, and how these intermediate pyrolysis products subsequently react to form char.

As is often done, we would like to be able to propose overall structures for the various residues. Although we have characterized the amount of sp^2 and sp^3 carbon and the amount of non-protonated carbon, an accurate representation is not possible without a more detailed knowledge of the CH to CH_2 ratio in these residues.

Poly(vinyl alcohol)/Bismaleimide Pyrolysis: On the basis of the above information, we attempted to enhance char formation in PVA, and reduce flammability, by increasing the opportunity for crosslinking and aromatization. We focused our efforts on reactions with the main condensed-phase decomposition products, the polyenes, generated from the chain-stripping elimination reaction. No attempt was made to prevent the chain-stripping elimination reaction itself, since it produces the nonflammable volatile, H_2O.

Since there is good evidence for reaction of the double bonds of the polyenes, we introduced thermally stable crosslinking additives that we hoped would react with the polyenes to form cyclohexenes faster than the polyenes either react with themselves or undergo chain scission. Ultimately for this to be successful such additives must also facilitate aromatization of the cyclohexenes to prevent the retro Diels-Alder reaction which is otherwise favored at high temperatures (*16*).

Bismaleimides are a class of reactive oligomers that undergo rapid reaction (Diels-Alder, Ene, etc.) above 200 °C with materials containing carbon-carbon double bonds. Bismaleimides have been employed as chain extenders, crosslinking and aromatization agents with many polymer and composite systems and as ingredients in the preparation of low flammability materials (*17*, *18*). The proposed reactions of these additives with the polyenes are shown in Figure 9. We examined PVA combined with each of the two bismaleimides shown in Figure 8. The bismaleimides, N,N'-1,4-phenylenedimaleimide (1,4-PDMI) and N,N'-1,3-phenylenedimaleimide (1,3-PDMI), were used to allow evaluation of the effect of structure on the bismaleimide's effectiveness. A monomaleimide, N-phenylmaleimide (PMI), was also included to compare chain branching or grafting to crosslinking.

Three mixtures, PVA/1,3-PDMI (10% by weight), PVA/1,4-PDMI (10%), and PVA/PMI (12%), were pyrolyzed in the N_2 flow pyrolysis furnace for 30 minutes at each of several temperatures. As was the case with PVA, the PVA/maleimide mixtures underwent the chain-stripping elimination of H_2O reaction and intumesced as they were heated. Figure 10 shows a plot of percent residue versus pyrolysis temperature for PVA and the PVA/maleimide mixtures. The presence of the maleimide has been factored out of these residue yields using nitrogen elemental analysis data. We assumed that the overall maleimide structure survived the pyrolysis and that the nitrogen remained intact in the imide. The PVA/maleimide mixtures all had higher residue yield relative to pure PVA at each pyrolysis temperature examined.

Pyrolysis at 300 °C. In general, if an additive can influence the decomposition process in the condensed phase at an early stage, the chances are improved for maintaining high char yields and for improving flammability properties. We focused our attention on characterizing the PVA/maleimide residues at 300 °C to determine how the maleimides improve the residue yields of PVA at this early stage in the decomposition, where a majority of the residue remains in the condensed phase.

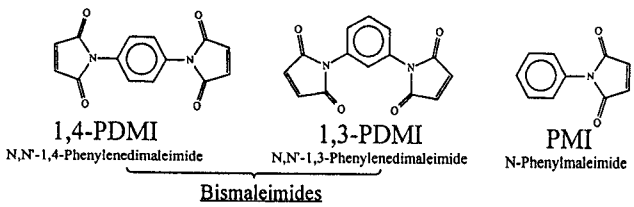

Figure 8. Structure of maleimides.

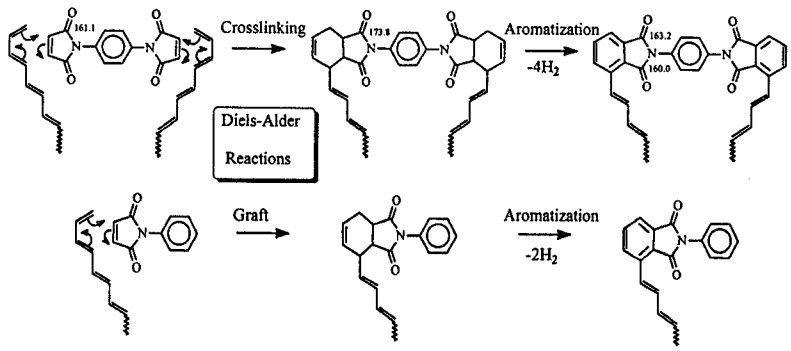

Figure 9. Diels-Alder reaction between polyene and maleimides and subsequent aromatization reactions.

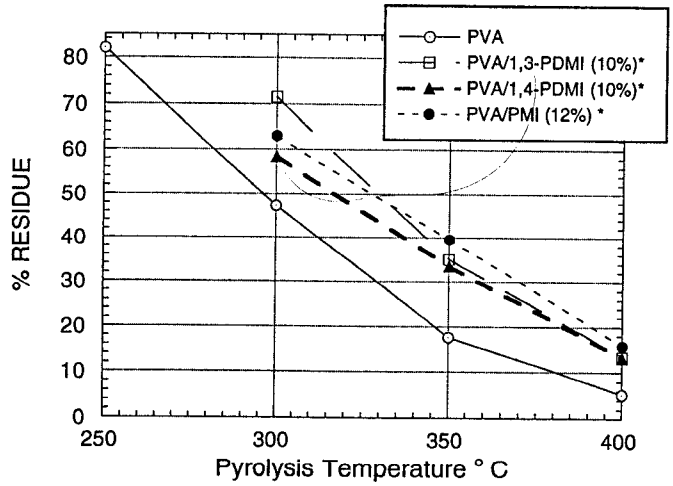

Figure 10. Plot of percent residue yield vs. pyrolysis temperature for PVA and PVA with each maleimide.The * indicates that the presence of the maleimide has been factored out of these residue yields using nitrogen elemental analysis data.

Figure 10 shows how the additives vary in their relative effectiveness at stabilizing PVA. The most effective maleimide is 1,3-PDMI whose mixture with PVA gives a 71.5% residue yield at 300 °C. The mixture of PVA and PMI gave a 67% residue yield. The mixture of PVA and 1,4-PDMI shows the smallest effect with a 58.4% residue yield. The residue yield for pure PVA was 47%.

As mentioned above the effectiveness of the maleimides as crosslinking agents for PVA depends on the degree of mixing. Differences in residue yields may be due to differences in solubility and/or melting point and their effect on additive/PVA mixing. 1,3-PDMI is very soluble in organic solvents and has a m.p. of 200 °C whereas 1,4-PDMI is nearly insoluble and has a m.p. > 350 °C due to its symmetrical structure. The monomaleimide, PMI, like 1,3-PDMI is also a very soluble compound it has a m.p. of 86 °C, and a boiling point of 300 °C. These differences indicate that 1,4-PDMI may not mix as readily with PVA as 1,3 PDMI or PMI, even at elevated temperatures.

Other effects, however, must also be examined. When considering any additive/polymer system the issue of additive loss through vaporization is an important and common concern, especially when the additive is designed to act in the condensed phase. If the additive has a significant vapor pressure at the temperature of exposure its' effectiveness will be compromised. The TGA, shown in Figure 11, shows a very different thermal response for the three maleimides; between 250 °C and 350 °C 1,4-PDMI experiences a rapid, 85% weight loss whereas 1,3-PDMI shows only a 20% weight loss. Observation of the heating of 1,4-PDMI using a hot plate melting point apparatus showed that the rapid weight loss for 1,4-PDMI may be due to sublimation since the only change seen was material loss. This difference in thermal response may explain the reduced effectiveness of 1,4-PDMI. Indeed, nitrogen elemental analysis shows that there was less imide (6.9%) in the PVA/1,4-PDMI residue than in the PVA/1,3-PDMI residue (9.2%). The TGA in Figure 11 shows, in contrast to 1,4-PDMI, 95% of PMI is lost before the temperature reaches 250 °C. However, PMI gives a 63% residue yield and it is present at 9.0% in the PVA/PMI residue. These data suggest that one factor controlling the effectiveness of the maleimides may be the competition between vaporization of the maleimide and solubilization and/or condensed phase reaction of the maleimide.

CP/MAS ^{13}C NMR Results. To attempt to determine how the maleimides improved the residue yields of PVA the residues were characterized using CP/MAS ^{13}C NMR. The CP/MAS ^{13}C NMR spectra, normalized to the same total intensity, of PVA, PVA 300 °C residue, and PVA/maleimide 300 °C residues are shown in Figure 12. For all of the PVA/maleimides pyrolyzed we see evidence of some sort of maleimide reaction. The spectrum of 1,4-PDMI is inset into Figure 12 and shows that the imide carbonyl signals typical of maleimide, at 164 and 175 ppm (which are split due to ^{13}C dipolar coupling to a ^{14}N quadrupolar nucleus), are converted to a single broad signal centered at 176 ppm (see predicted solution state imide-carbonyl ^{13}C chemical shifts in Figure 9) (*19*). Furthermore, in the aromatic region, 120-140 ppm, of Figure 12 we see the partially resolved resonances of crystalline 1,4-PDMI transformed into a broader resonance indicative of reaction and or a non-crystalline structure.

To gain additional insight into the effect the maleimides had on the PVA pyrolysis we sought to remove the resonances attributable to bismaleimide from the PVA/1,3-

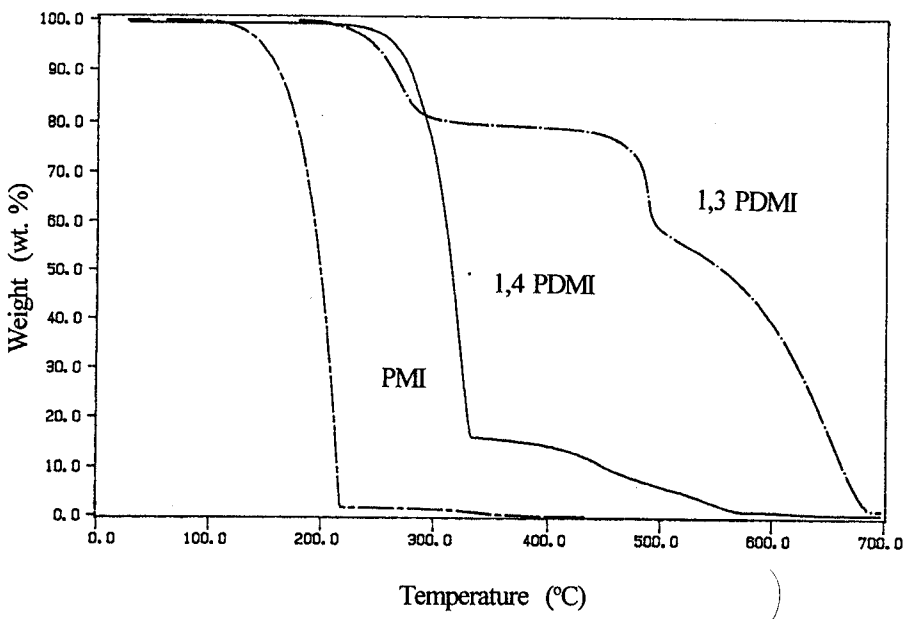

Figure 11. TGA of pure maleimides, 10 °C/min. Note that PMI experiences a rapid mass loss at low (< 200 °C) temperatures, 1,4 PDMI's mass loss is over 80% once the temperature has reached 350 °C, whereas 1,3 PDMI's mass loss is less than 50% even at 500 °C.

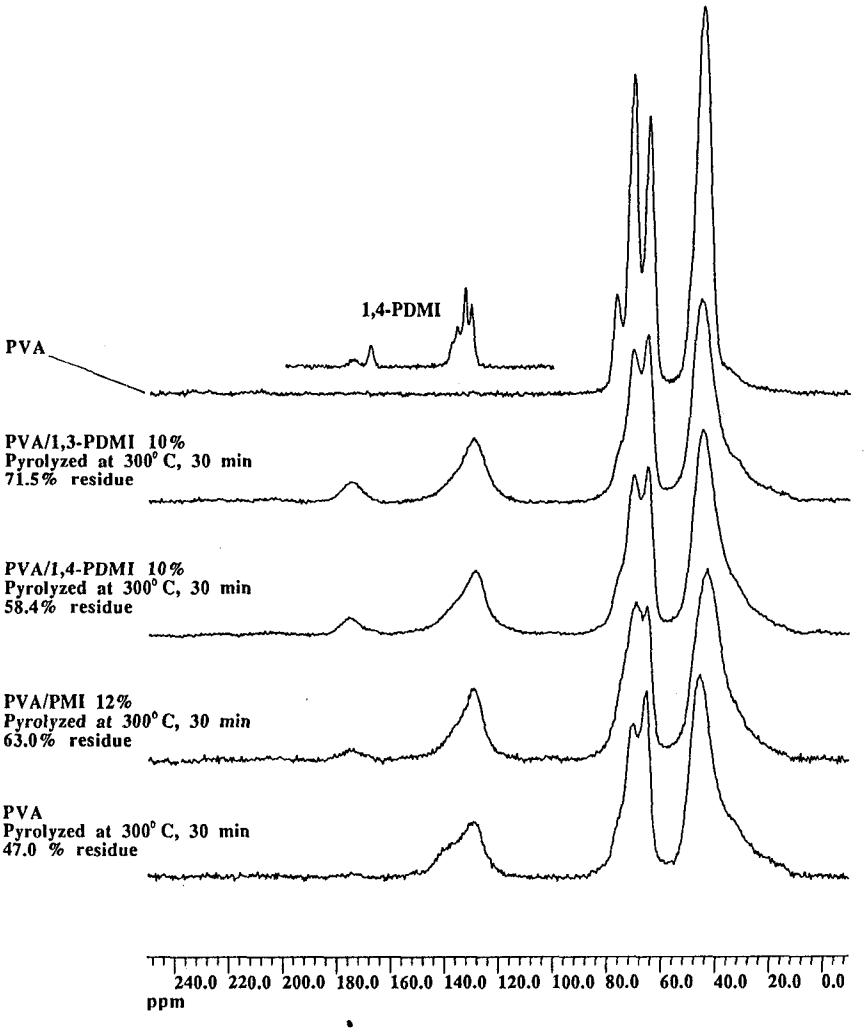

Figure 12. CP/MAS ^{13}C NMR spectra, normalized to the same total intensity, of pure 1,4 PDMI, PVA, three pyrolyzed (300 °C for 30 min) PVA/maleimide mixtures, and PVA pyrolyzed at 300 °C for 30 min. The broad peak near 172 ppm in the spectra of the mixtures arises primarily from the reacted maleimides; the aromatic/olefinic region (120-150 ppm) also contains a significant contribution from the maleimides.

PDMI residue spectrum. This allowed a more detailed comparison of the PVA/1,3-PDMI residue spectrum to the PVA residue spectrum, and was accomplished in the following manner: A sample of pure 1,3-PDMI was pyrolyzed in N_2 at 300 °C for 30 minutes, to give a residue yield of 80%. The idealized bismaleimide "homopolymer" structure, shown in Figure 13, is consistent with the spectrum of the residue from the pyrolysis of pure 1,3 PDMI shown on the bottom of Figure 14. This is based on the appearance and relative intensity of the aliphatic carbon signal centered at 45 ppm and a shift of the carbonyl band toward 175 ppm following pyrolysis. These two spectral features are consistent with polymerization at the double bond adjacent to the carbonyl. A shoulder remains at 170 ppm possibly indicative of the presence of unreacted maleimide carbonyl (~10%). The "corrected" PVA residue difference spectrum, shown at the top of Figure 14, was generated by subtracting the appropriate intensity of the "homopolymer" spectrum (bottom) from the PVA/1,3-PDMI residue spectrum (middle). The subtraction was done so that no intensity remained in the carbonyl region. The rationale which justifies doing this subtraction is based on the fact that the bissuccinimide repeat unit, shown in brackets in Figure 13, is common to both the homopolymer product and the product of the reaction of bismaleimides with polyolefins, as in Figure 9; hence, both the aliphatic and aromatic region of the homopolymer spectrum should give a good approximation of the spectral contributions resulting from reaction of 1,3-PDMI with unsaturation in PVA decomposition products. Also, no substantial carbonyl signals appeared in the pure PVA residue spectrum; therefore the main source of intensity in the carbonyl region should be from 1,3-PDMI.

Figure 15 shows a method of comparing the "corrected" PVA residue spectrum to the normal PVA residue spectrum where the intensities are scaled to their relative residue yields. This allows comparison of the residues on the basis of equal initial amounts of PVA. The resulting difference spectrum, shown on the bottom of Figure 14, appears to be that of intact PVA, indicating that less of the PVA has decomposed in the PVA/1,3-PDMI residue. Furthermore, integration of the normal PVA residue spectrum reveals that the ratio of alcohol carbon signal (-CHOH-) to the aromatic/olefinic carbon signal is 2.2 to 1. However, this ratio is 3.3 to 1 in the "corrected" PVA residue spectrum. Recalling that as pure PVA decomposes this ratio grows smaller and smaller until all the alcohol carbon signal is gone, as seen in Figure 3, these data confirm the fact that the PVA/1,3-PDMI residue is less decomposed than the normal PVA residue. These two samples, however, when compared on the basis of the same starting weight of PVA, contain the same amount of decomposition products (aromatics/olefinics at 120-140 ppm and aliphatics at 10-35 ppm), as evidenced by the nearly complete absence of these type of signals in the difference spectrum in Figure 14. An identical analysis of the 1,4-PDMI 300 °C residue spectra gave the same results.

It is not entirely obvious why, for a given initial amount of PVA, the PVA/1,3-PDMI residue shows the same amount of decomposition products as PVA does; yet, the overall residue yield is greatly increased.

An encapsulation mechanism involving bismaleimide may explain both the reduction in PVA decomposition and a greater retention of otherwise volatile decomposition products. The mechanism involves primarily a homopolymerization of the bismaleimide as a coating on the PVA, possibly accompanied by some crosslinking

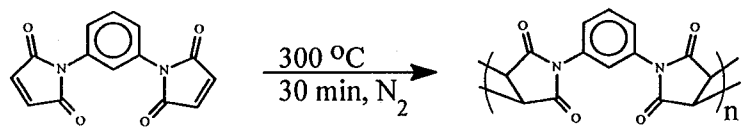

1,3-PDMI Bismaleimide "Homopolymer"

Figure 13. Proposed homopolymerization reaction of 1,3 PDMI, under the indicated conditions, to give the resulting bissuccinimide repeat unit in the polymer structure.

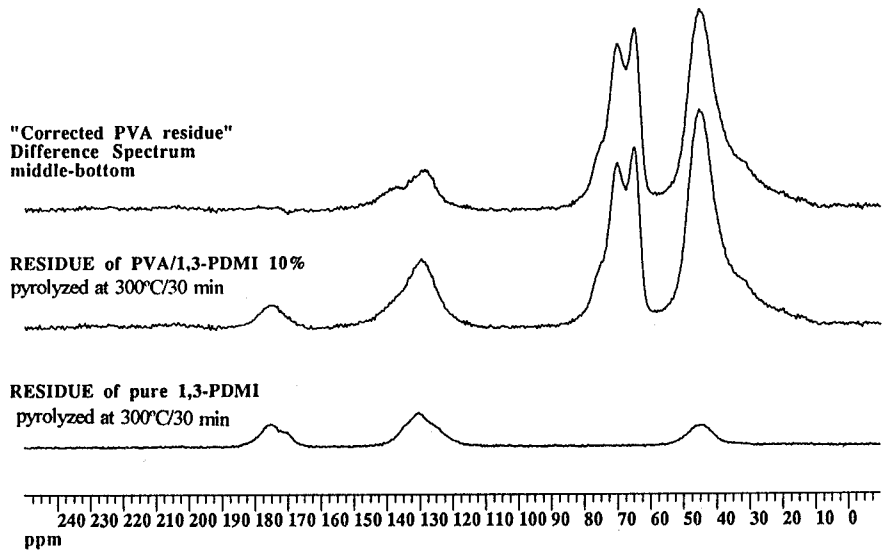

Figure 14. The "corrected" PVA residue difference spectrum (top) generated by subtracting the appropriate intensity of the "homopolymer" spectrum (bottom) from the PVA/1,3-PDMI 300 °C pyrolysis residue spectrum (middle).

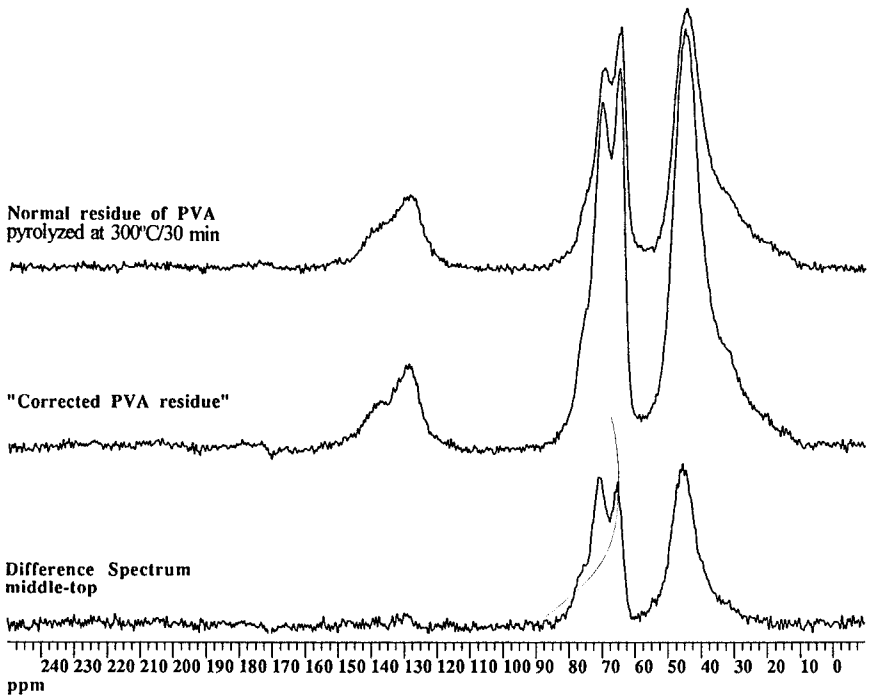

Figure 15. Comparison of the "corrected" PVA residue spectrum (middle) to the normal PVA residue spectrum (top) where the intensities are scaled to their relative residue yields. The resulting difference spectrum is shown on the bottom and appears to be that of intact PVA, indicating that less of the PVA has decomposed in the PVA/1,3-PDMI pyrolysis residue.

of PVA at the interphase between the two polymers. This highly crosslinked coating, similar in structure to the bismaleimide homopolymer shown in Figure 13, may act as a barrier preventing loss of volatiles, such as H_2O and chain-scission products, from the decomposing PVA. The existence of such a barrier may retard reactions, e.g., via Le Chatelier's principle, or it may force trapped volatiles to react with species in the condensed phase, i.e., with bismaleimide or other PVA decomposition products. In particular, it is possible that volatiles containing unsaturation reach the coating of partially polymerized 1,3-PDMI and are trapped in this layer by chemical reaction with maleimide functionality.

Relaxation Studies. We lack direct spectral evidence for reaction of 1,3-PDMI with PVA or its decomposition products. We really only know that most of the imide carbonyls in the PVA/1,3-PDMI residue spectrum are adjacent to sp^3 instead of sp^2 carbons following the pyrolysis. Since the mechanistic mode of action for the maleimides was envisioned to be chemical rather than physical and therefore depended on how well the maleimides mixed with PVA, it seemed relevant to inquire qualitatively about the level of mixing of the maleimides with PVA.

Given the structural differences between the maleimides and PVA we might anticipate differences in intrinsic relaxation times for protons in these compounds. One can use either the rotating frame proton relaxation time, $T_{1\rho}^H$, or the longitudinal proton relaxation time, T_1^H, as a time scale over which heterogeneity of composition is probed. Proton spin diffusion is a transport property (*20*) of spin polarization which tends to keep polarization per spin uniform in a given locale. In contrast, local differences in relaxation times promote the production of polarization gradients. If, for example, on the time scale of the shortest observed $T_{1\rho}^H$ (~5 ms) or a time scale like 0.75 s which is of the order of T_1^H, spin diffusion is not capable of keeping polarization/spin equal, then one can infer heterogeneity of composition on a distance scale related to these times. Distances of polarization transport are as follows; 5 ms in $T_{1\rho}^H$ corresponds to ~ 1.5 nm, and 0.75 s in T_1^H corresponds to ~ 27 nm. Since domains have boundaries on at least two sides, spin diffusion can usually cover a domain about twice these characteristic dimensions in such a time (*21*). Lineshape changes in spectra due to differences in $T_{1\rho}^H$ or T_1^H behavior suggest domains bigger than, about, two-thirds of such domain sizes, i.e., 2 nm for a $T_{1\rho}^H$ of 5 ms and 36 nm for T_1^H of 0.75 s.

We found the following results and offer the corresponding interpretations. First, in the pure PVA 300 °C residue there was an inhomogeneity on a T_1^H scale of 0.75 s; PVA decomposition products had a shorter T_1^H. Hence on a 36 nm scale or above, the PVA degradation was not homogeneous. For the PVA/1,3-PDMI residue, the carbonyl region (mainly from 1,3-PDMI) relaxed at a different rate (on a scale of 0.75 s) than did PVA-related resonances, including some intensity in the 120-140 ppm range. Figure 16 shows two spectra taken at different repetition times along with the difference spectrum. (The experimental spectra result from different number of scans; however, they are normalized to the same number of scans.) The absence of a signal in the difference spectrum in the carbonyl region, where 1,3 PDMI contributions dominate, indicates that most of the pyrolysis products of the 1,3 PDMI are in a region where T_1^H is less than 300 ms. The meaning of the difference spectrum in Figure 16 is that there are regions of the sample, which give rise to these resonances, where T_1^H 's are significantly longer than 300 ms. Included in these later regions one can find PVA

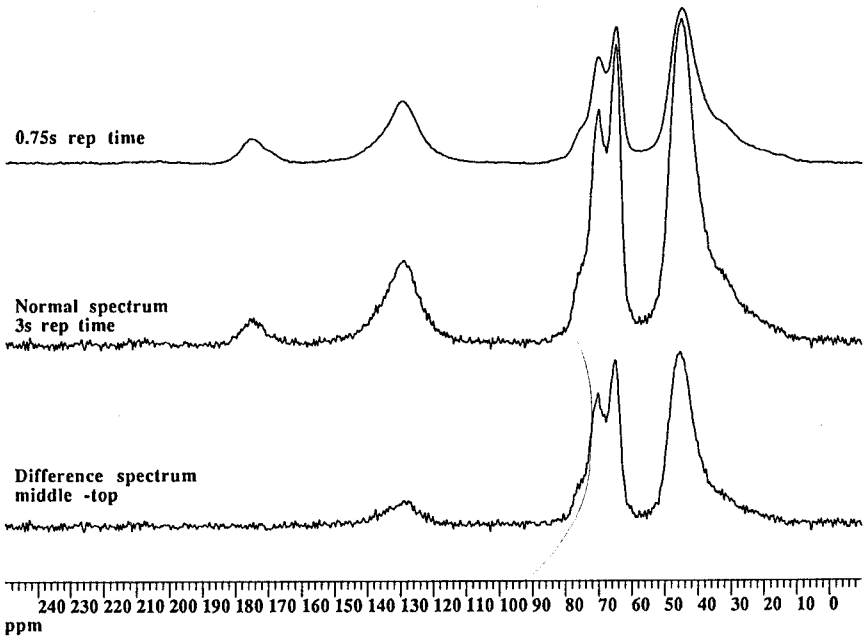

Figure 16. Comparison of CP/MAS ^{13}C NMR spectra of PVA/1,3 PDMI pyrolyzed at 300 °C for 30 min taken at different repetition times (as indicated) and the difference spectrum (bottom). The different lineshapes indicate a chemical inhomogeneity on a scale larger than 36 nm. The disappearance of the maleimide line at 172 ppm in the difference spectrum points to a significant, albeit not necessarily complete, phase separation of the maleimide phase.

olefinic/aromatic decomposition products (120-140 ppm) as well as resonances associated with undegraded or mildly degraded PVA. It should be clearly understood that the data in Figure 16 prove the inhomogeneous mixing of the 1,3 PDMI pyrolysis products; on the other hand, these data are insufficient to show whether partial mixing between PVA and 1,3 PDMI occurred. If there were only two kinds of chemically distinct regions in the sample, one might be able to address this question. Given the chemical inhomogeneities in the pyrolysis products of pure PVA cited above, one might expect three or more regions of chemical inhomogeneity in this sample. It would require a lot more data to sort out the spectra corresponding to each region. We will not attempt to determine whether some PVA pyrolysis products are spatially proximate to the pyrolysis products of 1,3 PDMI, even though this is an interesting question. Suffice it to say that the inhomogeneous mixing of the 1,3 PDMI pyrolysis products demonstrates that PVA and 1,3 PDMI melts are either not highly miscible or that the homopolymerization of PDMI or the pyrolysis of PVA prevents full mixing. Since the proposed mechanism of chemical intervention by maleimide, with the PVA decomposition products, requires thorough mixing of ingredients, we must maintain considerable skepticism that 1,3-PDMI is available to completely react with all of the sites of PVA decomposition. One should bear in mind, however, that even a partial solubility might be efficacious in reducing the decomposition rate of PVA particularly if the elimination of H_2O is autocatalytic, that is, if the presence of unsaturation from a previous elimination reaction, adjacent to an alcohol, accelerates subsequent elimination. Then reaction of even small quantities of bismaleimide with this unsaturation could significantly slow the rate of chain-stripping elimination.

For the PVA/1,4-PDMI 300 °C residue inhomogeneities are also visible on 36 nm or larger scale. For the PVA/PMI 300 °C residue inhomogeneities at the 36 nm scale were by comparison quite minor, although inhomogeneities were evident on the 2 nm scale via $T_{1\rho}^{H}$ experiments. An important perspective on these T_1^H experiments is that inhomogeneities can be demonstrated only when the intrinsic T_1^H 's in the different regions have contrast with one another. Hence the absence of contrast in the PVA/PMI 300 °C residue spectra on a 0.75 s time scale does not automatically imply that mixing is homogeneous on the 36 nm scale. However, as noted previously, the level of retention of PMI derived products in the PVA/PMI 300 °C residue implies that PMI penetrated the PVA in significant amounts and that it mixed more thoroughly with PVA or its decomposition products than did the other maleimides.

Residue Morphology. Examination of the morphology of the residues supports the above observations. Visual inspection, using an optical stereo-microscope (30X), of the PVA 300 °C residue shows a continuous crosslinked, multi-cellular, glassy, tan-colored foam, a material which at this scale appears reasonably homogeneous except for the bubbles. PVA/1,3-PDMI residue, however, looks somewhat heterogeneous. It is made up primarily of a fused mass of 1-3 mm size foam spheres mixed with and coated by dense glassy reddish-brown material. The presence of two different morphologies supports the notion that the bismaleimide and PVA melts are not highly miscible. The formation of the foam spheres implies that the PDMI caused isolation (e.g., by melt wetting in the case of 1,3 PDMI or sublimation in the case of 1,4 PDMI) of PVA particles from one another. If the PDMI formed a melted coating on each PVA particle,

then as the coating crosslinked it would behave as an elastomer allowing expansion of the molten particle as the PVA decomposes and generates volatiles. Finally, expansion might cease when the crosslink density got too high.

The morphology of the PVA/1,4-PDMI residue is similar to that of the PVA/1,3-PDMI residue except the foam spheres are not fused together at all and are only lightly "frosted" by a small fraction of the dense glassy reddish-brown material. We were actually able to separate the foam spheres and dense glassy materials by sieving (80 mesh). CP/MAS ^{13}C NMR analysis, similar to that done with the PVA/1,3-PDMI residue (i.e., Figure 14), revealed that the foam spheres (89% of the residue) were less decomposed than the dense glassy reddish-brown material (11% of the residue) even though the foam spheres contained less 1,4-PDMI residue (~4%, by elemental analysis) than the dense glassy reddish-brown material (~37%, by elemental analysis). This appeared, at first, quite puzzling and antithetical to our proposed encapsulation mechanism. It is, however, consistent with our explanation if one considers the possibility that PVA's decomposition products, especially those with lower molecular weight, like those shown in Figure 2, are more miscible with the 1,4-PDMI melt than PVA itself is, and that more extensive PVA decomposition in this material may be explained by a trapping of the decomposition products via chemical reaction with maleimide functionality. To determine, however, if the higher concentration of PVA decomposition products in the additive rich portion of the residue was due to degradation of PVA in the presence of high concentrations of additive, we pyrolyzed a PVA with 36% 1,3-PDMI. The corrected residue yield was in fact 78%, an increase of 7% relative to pyrolyses using 10 % of this bismaleimide. An analysis of the PVA/1,3-PDMI(36%) residue spectrum identical to that done for the PVA/1,3-PDMI(10%) residue, i.e., as in Figures 14 and 15, showed that overall, less PVA decomposes in the presence of the higher level of additive and that when the spectra are normalized to the same starting weight of PVA in the mixture, more decomposition products were present in the PVA/1,3-PDMI(36%) residue. The higher level of decomposition products present supports the idea that they are more miscible with and more easily trapped by the bismaleimide portion of the residue.

The PVA/PMI residue appears much more homogeneous than the PVA/bismaleimide residues and is comparable to the dense reddish-brown material present in the other PVA/bismaleimide residues with a small amount of entrapped bubbles. This morphology supports the implication that PMI mixed more thoroughly with PVA and its decomposition products than did the bismaleimides. However, more thorough mixing did not result in as strong an increase in residue yield as would be expected if molecular accessibility to the maleimide functionality was important to retarding PVA decomposition. Perhaps this relates to the monofunctional rather than difunctional structure of the PMI relative to the PDMI's. Although monofunctionality appears sufficient to retain most of the PMI in the residue. On the other hand, if the PMI is much more accessible for reaction with sites of unsaturation caused by water loss from PVA, then the extent of PVA decomposition observed tends to question the idea that maleimide reaction can arrest an autocatalyzed chain-stripping reaction, unless PMI reacts with itself in preference to reaction with unsaturation at PVA sites. A more likely scenario is that the maleimides react with unsaturation in PVA decomposition products, thereby lowering their average volatility. Whether this happens in the region

where the decomposition initially takes place, as it may in the PVA/PMI mixture, or by having unsaturated volatiles get trapped by reaction in a phase-separated domain, as is likely in the PVA/PDMI mixtures, the net effect on residue yield is similar.

Gasification and Cone Calorimetry. The goal of this research was to characterize the fundamental condensed phase processes and structures which lead to char formation during polymer pyrolysis and to use this information to design new strategies which increase char formation and improve polymer flammability properties. An increase in char yield at intermediate temperatures, although promising, does not guarantee a like improvement in combustion char yield or flammability properties. To evaluate the "real" effect the maleimides have on PVA flammability we exposed PVA and two of the PVA/maleimide mixtures to fire-like non-oxidizing conditions in a gasification apparatus which exposes compression molded samples (40g, disks) to a radiant heat source similar to that experienced by materials in a real fire, 40 kW/m^2, in a N_2 atmosphere. The results, shown in Figure 17, reveal a significant reduction in the maximum mass loss rate for the PVA/1,3-PDMI and PVA/PMI mixtures as compared to PVA alone. The strongest effect, that of 1,3-PDMI, was a 20% increase in the time to complete pyrolysis. However, the final char yields were all very similar, ~ 5%.

Comparison of the flammability of PVA and the PVA/1,3-PDMI mixture was done in a Cone Calorimeter. This apparatus also exposes compression molded samples (40g, disks) to a radiant heat source (40 kW/m^2), but the sample is exposed to the air and is ignited by a spark source. As would be expected from the above results, there was a delay in the "time of peak heat release," 367 ± 18 seconds for PVA/1,3-PDMI versus 222 ± 33 seconds for PVA alone. However, there were no other significant differences in the flammability behavior for PVA as compared to the PVA/1,3-PDMI mixture (mean heat release rate ~ 470 kW/m^2, total heat released ~ 170 MJ/m^2, heat of combustion ~ 19 MJ/kg). The char yield, however, was slightly increased from 3% to 5% by the presence of 1,3-PDMI.

Conclusions

CP/MAS ^{13}C NMR analysis has allowed characterization of the condensed phase processes which occur during the pyrolysis of PVA and PVA combined with maleimides. The maleimides effect a stabilization of the PVA at 300-400 °C. Although this stabilization improves the pyrolysis residue yields in the 300-400 °C regime, it does not significantly increase the char yields under combustion or high temperature (700-800 °C) pyrolysis conditions. Presumably, this is due to the fact that the maleimides' primary modes of action are physical encapsulation and a lowering of the average volatility (probably by chemical trapping) of certain degradation products as opposed to the formation of thermally stable aromatic crosslinks as was initially envisioned. The moderate increase in "time of peak heat release" resulting from the addition of maleimide, might be viewed as useful if it provided enough of a delay to allow a formulation or product to pass an application specific fire test. However, the results obtained here might be significantly different when reduced to practice in bulk materials, since the effectiveness of the physical encapsulation mechanism depends upon coating the surface of particles, and such a morphology

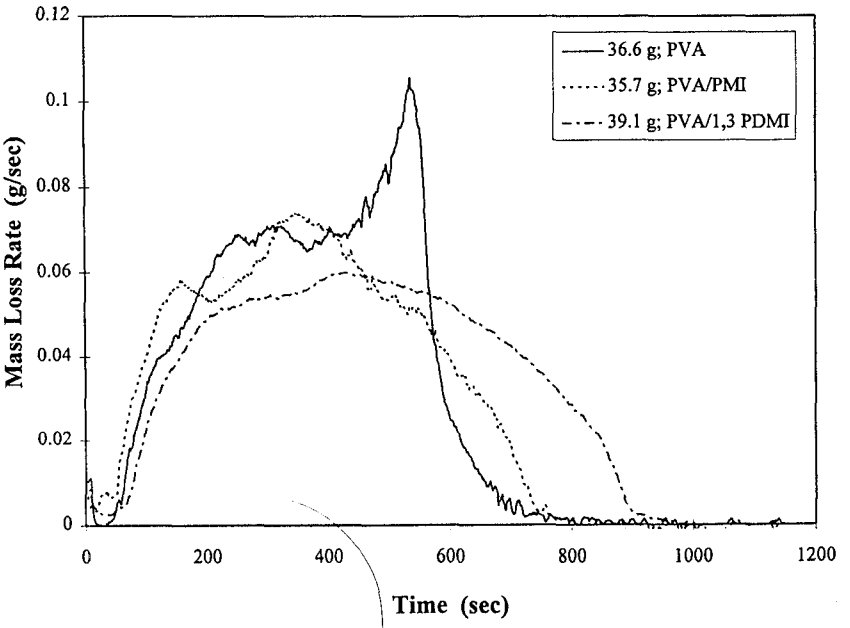

Figure 17. Plot of mass loss rate vs. time for the high temperature (700-800 °C) pyrolysis of PVA, PVA/PMI, and PVA/ 1,3 PDMI in a gasification apparatus which exposes samples (40g, disks) to a high intensity radiant heat source (40 kW/m^2), in a N_2 atmosphere.

would not exist in a bulk material. On the other hand a mechanism which reduces the volatility of degradation products might maintain its effectiveness and impart some protection to the bulk. To gain a greater reduction in flammability, however, will require a more through understanding of and control over the condensed phase chemistry.

Acknowledgements

The authors are grateful for the skillful assistance of Mr. Michael Smith, Mr. Jack Lee, and Mr. John Shields. We also thank Dr. Phil Austin for the gasification apparatus work and Dr. Barry Bauer for use of the TGA.

Literature Cited.

1. Dumler, R.; Lenoir, D.; Thoma, H. and Hutzinger, O. *Journal of Analytical and Applied Pyrolysis*, **1989**, 16, pp 153-158.
2. Lindsay, K. F. *Modern Plastics*, February, **1994**, p 54.
3. Van Krevelen, D.W. *Polymer*, **1975**, *vol 16*, pp 615-620.

4. Brauman, S. K. *J. of Fire Retardant Chemistry*, November, **1979**, *vol 6*, pp 248-265.
5. Tubbs, R. K.; Wu, T. K. In *Poly(vinyl alcohol), Properties and Applications;* Finch, C.A., Ed.; John Wiley & Sons: London, 1973, chapter 8.
6. Zhang, X.; Takegoshi, K. and Hikichi, K. *Polymer*, **1992**, vol 33, pp 718-724.
7. Certain commercial equipment, instruments, materials, services or companies are identified in this paper in order to specify adequately the experimental procedure. This in no way implies endorsement or recommendation by NIST.
8. Brauman, S. K.; *J. of Fire Retardant Chemistry*, November, **1979**, *vol 6*, pp 266-275.
9. O'Donnell, D. J. In *NMR and Macromolecules, Sequence, Dynamic, and Domain Structure;* Randall, J. C. Jr., ED.' ACS Symposium Series 247; American Chemical Society, Washington, D. C. 1984; pp 21-41.
10. Opella, S. J.; Frey, M. H. *J. Am.Chem.Soc.* **1979**, *vol 101*, p 5854.
11. Cullis, C.F.; Hirschler, M.M. *The Combustion of Organic Polymers,* Clarendon Press, Oxford, 1981, pp 117-119.
12. Anders, H.; Zimmerman, H. *Polymer Degradation and Stability*, **1987**, *vol 18*, pp 111-122.
13. Muruyama, K.;Takeuchi, K. and Yanizaki, Y. *Polymer,* March, **1989**, *vol 30*, pp 476-479.
14. Cullis, C.F.; Hirschler, M.M.*; The Combustion of Organic Polymers,* Clarendon Press, Oxford, 1981, pp 143-145.
15. ^{13}C NMR assignments taken from: Kalinowski, H. O.;Berger, S. and Braun, S. *Carbon-13 NMR Spectroscopy*, 1988, John Wiley & Sons Ltd., Eds.; pp 132-203., and C-13 Module for Chem Windows, Softshell International software program, version 3.02.
16. Sauer, J.; Sustmann, R. *Angew. Chem.,Int. Ed. Engl.* **1980**,*vol 19*, p 779.
17. Gruffaz, M.; Rollet, B. *U.S. Patent 4,016,114*, April 4, 1977.
18. Carduner, K. R.; Chattha, M. S. In *Crosslinked Polymers, Chemistry, Properties and Applications*, ACS Symposium Series, American Chemical Society, Washington, D. C., 1987, Vol. 367, pp 379-380.
19. VanderHart, D. L.; Tan, L. S. *Materials Research Society Symposium Proceedings*, **1989**. *vol 134*, p 560.
20. Abragam, A. *The Principles of Nuclear Magnetism;* Oxford University Press: London, 1961; Chapter V.
21. Havens, J. R.; VanderHart, D. L. *Macromolecules*, **1985**, *vol 18*, p 1663.

RECEIVED March 31, 1995